

University of Rhode Island

DigitalCommons@URI

Open Access Master's Theses

2013

Developing a Method for Enhanced Explosive Detection by Surface Enhanced Raman Scattering (SERS) and Metal Enhanced Fluorescence (MEF)

Meredith A. Matoian

University of Rhode Island, meredithmatoian@gmail.com

Follow this and additional works at: <https://digitalcommons.uri.edu/theses>

Terms of Use

All rights reserved under copyright.

Recommended Citation

Matoian, Meredith A., "Developing a Method for Enhanced Explosive Detection by Surface Enhanced Raman Scattering (SERS) and Metal Enhanced Fluorescence (MEF)" (2013). *Open Access Master's Theses*. Paper 4.

<https://digitalcommons.uri.edu/theses/4>

This Thesis is brought to you by the University of Rhode Island. It has been accepted for inclusion in Open Access Master's Theses by an authorized administrator of DigitalCommons@URI. For more information, please contact digitalcommons-group@uri.edu. For permission to reuse copyrighted content, contact the author directly.

DEVELOPING A METHOD FOR ENHANCED
EXPLOSIVE DETECTION BY SURFACE ENHANCED
RAMAN SCATTERING (SERS) AND METAL
ENHANCED FLUORESCENCE (MEF)

BY

MEREDITH A. MATOIAN

A THESIS SUBMITTED IN PARTIAL FULFILLMENT OF THE
REQUIREMENTS FOR THE DEGREE OF
MASTERS OF SCIENCE
IN
CHEMISTRY

UNIVERSITY OF RHODE ISLAND

2013

MASTER OF SCIENCE
OF
MEREDITH A. MATOIAN

APPROVED:

Thesis Committee:

Major Professor Dr. William B. Euler

Dr. Michael Greenfield

Dr. Sze Yang

Nasser H. Zawia
DEAN OF THE GRADUATE SCHOOL

UNIVERSITY OF RHODE ISLAND
2013

ABSTRACT

The first manuscript, “Fabrication of SERS Substrates for Explosive Detection,” focuses on the development of a Surface Enhanced Raman Scattering (SERS) substrate for use in the area of explosive detection. The substrate was created by immersion plating of silver onto porous silicon, resulting in a Ag roughened surface with an average roughness of 135 nm as determined by AFM. When explosive solutions, such as trinitrotoluene (TNT) and dinitrotoluene (DNT) in ethanol, were applied directly to the substrate, detection of unique Raman bands was possible down to the $10^{-9} - 10^{-10}$ mol/cm² range. These results prove the technique is selective and shows promise for future work when vapor phase explosives will be investigated.

The second manuscript entitled “Light Trapping to Amplify Metal Enhanced Fluorescence with Application for Sensing TNT” focuses on the use of the previously mentioned substrate for Metal Enhanced Fluorescence (MEF). By using a polymer layer as a dielectric spacer in between the Ag layer and the fluorophore, enhancement of fluorescent emission was possible even though the spacer thicknesses was 10 – 20 times larger than typically reported. In experiments with rhodamine 6G, the fully assembled substrate resulted in a 1600-fold enhancement of emission. Compared to the usually reported $10^1 - 10^2$ times enhancement, the large enhancement is suspected to occur due to numerous effects. As enhancements were observed with and without the roughened Ag layer, light trapping is suggested as a contributing factor in addition to MEF. While less effective in enhancing the emission of the conjugated polymer

methoxy-ethylhexoxypolyphenylene-vinylene (MEH-PPV) that is known to interact with TNT vapor, the quench in fluorescent emission of MEH-PPV occurred more rapidly when the light trapping polymer was incorporated. Rapid detection and increased sensitivity are important features to the detection of trace explosives.

ACKNOWLEDGMENTS

I would first like to acknowledge everyone in the Euler research group, specifically my research advisor, **Dr. William Euler**. When Dr. Euler suggested I fulfill my undergraduate research requirements in his group, I had no idea my interest in the area would lead to graduate school. Thank you for providing me with the opportunity and guidance. Also, thank you to **Dr. Christopher Latendresse** for dealing with me on a daily basis, ensuring a good experience in this stressful setting, and providing a wealth of knowledge. To **Emily Hall, Richard Sweetman, Courtney McGowan, Hui Qi Zhang,** and **Shayna Albanese**: I appreciate all the hard work! Your assistance in this project was vital. I am also grateful for the guidance and education provided to me by the past members of the Euler research group, specifically **Dr. Drew Brodner**. I could not have done this without each and every one of you.

Finally, I would like to thank my family for all of their love and support. Without the encouragement of my parents, **Mark** and **Jayne Matoian**, my sister, **Hillary Lesperance**, and brother-in-law, **Dana Lesperance**, this goal would not have been possible.

PREFACE

The manuscript format outlined by the Graduate School at the University of Rhode Island will be utilized for the presentation of this thesis. Two manuscripts will make up the thesis.

The first manuscript is entitled “Fabrication of SERS Substrates for Explosive Testing.”

The second manuscript that is entitled “Light Trapping to Amplify Metal Enhanced Fluorescence with Application for Sensing TNT” will be submitted in 2013.

TABLE OF CONTENTS

| | |
|---|------|
| ABSTRACT | ii |
| ACKNOWLEDGMENTS | iv |
| PREFACE | v |
| TABLE OF CONTENTS | vi |
| LIST OF TABLES | viii |
| LIST OF FIGURES | ix |
| LIST OF SCHEMES | x |
| INTRODUCTION | 1 |
| References | 5 |
| MANUSCRIPT 1 | |
| Fabrication of SERS Substrates for Explosive Testing..... | 6 |
| Abstract | 7 |
| Introduction | 7 |
| Experimental | 9 |
| Results and Discussion..... | 12 |
| Conclusions | 22 |
| References | 23 |
| Supplementary Information | 24 |
| MANUSCRIPT 2 | |
| Light Trapping to Amplify Metal Enhanced Fluorescence with Application for Sensing TNT | 25 |
| Abstract | 26 |

| | |
|-----------------------------|----|
| Introduction | 26 |
| Experimental | 27 |
| Results and Discussion..... | 29 |
| Conclusions | 36 |
| References | 38 |

LIST OF TABLES

| TABLE | PAGE |
|--|------|
| Manuscript 1 | |
| Table 1. Raman peaks for each analyte assigned to specific structural features, where “sh” represents shoulder. The resolution of the instrument is 4 cm^{-1} | 22 |
| Supplementary Information | |
| Table 1. Further height parameters for the AFM image of p-Si/Ag sample seen in Figure 3 | 24 |

LIST OF FIGURES

| FIGURE | PAGE |
|--|------|
| Manuscript 1 | |
| Figure 1. Raman spectra of Rh6G on p-Si/Ag substrates with varying length of Ag growth | 14 |
| Figure 2. The average Raman intensity of 4.3×10^{-10} mol/cm ² Rh6G at 1517 cm ⁻¹ was plotted versus Ag growth time. | 15 |
| Figure 3. AFM image of a 5 μ m by 5 μ m region of a p-Si/Ag substrate..... | 16 |
| Figure 4. XPS data collected from a p-Si/Ag sample | 17 |
| Figure 5. Raman spectra obtained of Rh6G on p-Si/Ag substrates used to determine the limit of detection of the Agilitron instrument. | 18 |
| Figure 6. Raman intensity obtained of Rh6G at 1517 cm ⁻¹ on p-Si/Ag substrates used to determine the limit of detection of the Agilitron instrument. | 19 |
| Figure 7. SERS spectra of explosive analytes on p-Si/Ag substrates. | 21 |
| Manuscript 2 | |
| Figure 1. Emission spectra of Rh6G coated on different polymers cast on a p-Si/Ag substrate..... | 30 |
| Figure 2. Emission spectra of Rh6G coated on different polymers cast on a glass substrate (upper) and a flat Si substrate (lower)..... | 31 |
| Figure 3. Emission spectra of Rh6G cast on PVDF with different substrates | 33 |
| Figure 4. Reflection spectra | 34 |
| Figure 5. Quenching of MEH-PPV at λ_{\max} (598 nm) upon exposure to TNT..... | 36 |

LIST OF SCHEMES

| SCHEME | PAGE |
|--|------|
| Introduction | |
| Scheme 1. Schematic of suggested explosive sensor..... | 3 |
| Manuscript 1 | |
| Scheme 1. Analytes used for explosive studies | 10 |
| Manuscript 2 | |
| Scheme 1. Varying substrate assemblies utilized in this study to demonstrate the enhancement of fluorescent emission | 26 |

INTRODUCTION

Work to create an effective sensor for the detection of explosives has been ongoing for the past few decades. Having impact in both national security and environmental safety, the need for a sensitive and selective sensor is still relevant as acts of terrorism continue and landmines remain undiscovered. Explosive analytes, which have typically low vapor pressures, present many difficulties in the field of detection, requiring novel ideas for improvement. The goal is to create a sensor with very low detection limits that is also portable, accurate and rapid.

Varying approaches have been considered to solve the problem of undetected explosives. Most notably, canine detection teams, colorimetric techniques, ionization mass spectrometry (IMS), and fluorescence have been employed. Able to discern individual scents even when masked by other chemicals, trained canines have proven to be one of the more effective techniques.¹ Unfortunately, training of these dogs and their accompanying law enforcement personnel is very expensive. Other methods strive to achieve similar levels of sensitivity while decreasing cost and reliance on personnel. For example, colorimetric sensors rely on chemical reactions between an indicator and explosive residues to alter absorbance. This method is portable, easy to interpret and sensitive.¹ IMS is also accurate to low levels of explosive residue, but the instrument is not typically portable making it less attractive for field work.¹ Finally, fluorescence techniques are frequently utilized for explosive sensors. The most successful example is Fido, an explosive sensor patented by Dr. Timothy Swager at MIT involving a flat substrate with a conjugated fluorescent polymer.^{2,3} As

explosive analytes themselves are not known to fluoresce, reporter molecules like the conjugated polymer selected by Swager are incorporated into sensors. The reporter molecule is a fluorophore that has a known interaction with the analyte of interest, causing a quench or enhancement in the fluorescence emission that indicates a positive test result. Fido reportedly can detect levels as low as one femtogram of TNT through this approach³, proving that fluorescence methods are sensitive and applicable to a portable sensor.

In the past, this research group has approached the detection of explosives from the sole perspective of fluorescence. Working with EmiTech Inc., an explosive sensor was created utilizing a porous silicon substrate for increased surface area and a conjugated polymer acting as the fluorescent reporter molecule.^{4,5} While this method has been proven to be sensitive to a few explosives, this established sensor and others of its kind could benefit from added selectivity. Because many vapors can be responsible for a quench or enhancement of fluorescence emission, another complementary spectroscopic technique is needed.

Combining the sensitive fluorescence technique with Surface Enhanced Raman Scattering (SERS) will increase the selectivity of the sensor with additional information. SERS is a technique that utilizes a roughened metal layer to amplify Raman signals that provide important vibrational information. Because each molecule has a unique structure, an individual spectrum is possible for each explosive analyte of interest. As a result, any sensor that incorporates SERS is inherently selective, allowing for identification of an unknown. The technique has also proven to be sensitive with single molecule detection possible.^{6,7} Enhancements on the order of

10^3 - 10^6 are typical^{8,9}, relying on the morphology of the metal surface. Optimization of the substrate is vital to an effective SERS sensor.

Utilizing a similar substrate, fluorescence signals can also be enhanced for increased sensitivity. The phenomenon known as Metal Enhanced Fluorescence (MEF) requires a spacer of 50 – 100 Å^{10,11} thickness between the selected fluorophore and the metal layer. Once optimized and assembled, enhancements on the order of 10^1 - 10^2 are reported. By establishing an appropriate spacer and utilizing the same metal substrate as the SERS experiments, the explosive sensor can also improve in sensitivity.

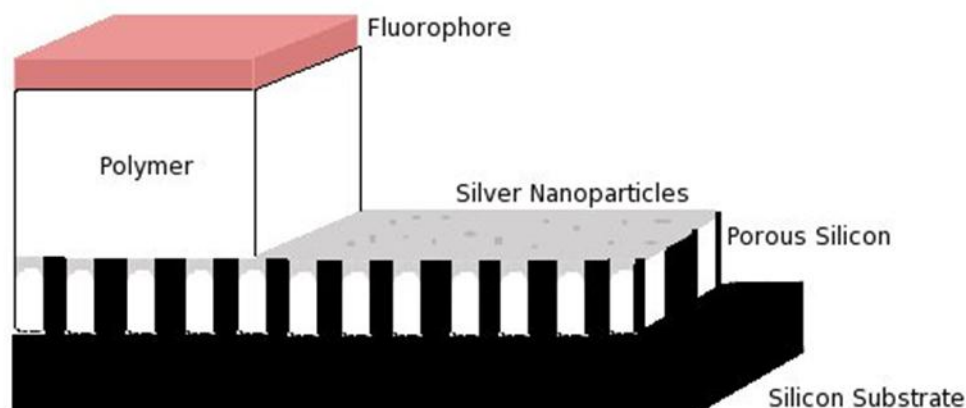


Figure 1. Schematic of the suggested explosive sensor.

In order to capitalize on the enhancements in sensitivity and selectivity provided by SERS and MEF, a combined sensor is suggested for the detection of explosives. Figure 1 represents the proposed sensor. Starting at the right side of the sensor, the flat silicon region will provide an area for background data to be collected if needed. The center portion, made of a simple porous silicon and Ag nanoparticle (p-Si/Ag) assembly, can be utilized for SERS. The left edge of the sensor will be

reserved for MEF experiments, comprised of the same p-Si/Ag substrate, a polymer spacer and a fluorophore with known interactions to explosives.

The manuscripts presented herein discuss preliminary research that has been done in this effort. Manuscript 1 presents the procedure and characterization of the p-Si/Ag substrate. Also, included SERS spectra of varying explosives show that detection is possible utilizing the substrate. The second manuscript shows that large enhancements in fluorescence are possible through the suggested MEF substrate. Continuing work will be needed to take this sensor a step further, establishing an array sensor capable of discerning a variety of explosive vapors in the field.

References

1. Germain, M.E.; Knapp, M.J.; *Chem. Soc. Rev.*, **2009**, 38, 2543 – 2555.
2. Thomas, S.W.; Joly, G.D.; Swager, T.M.; *Chem. Rev.*, **2007**, 107, 1339-1386.
3. <http://gs.flir.com/detection/explosives/fido> (accessed Aug. 1, 2012).
4. http://www.emitechinc.com/chem_nanosensors.html (accessed Nov. 1, 2012).
5. Levitsky, I. A.; Euler, W. B.; Tokranova, N.; and Rose, A.; *Appl. Phys. Lett.*, **2007**, 90, 041904/1 – 041904/3.
6. Nie, S.; Emory, S. R.; *Science*, **1997**, 275, 1102 – 1106.
7. Otto, A.; *J. Raman Spectrosc.*, **2002**, 33, 583 – 598.
8. Jerez-Rozo, J.I.; Primera-Pedrozo, O.M.; Barreto, Cabán, M.A.; Hernández-Rivera, S.P.; *IEEE Sens. J.*, **2008**, 8, 974 – 982.
9. Skoog, D.A.; Holler, F.J.; Crouch, S.R.; *Principles of Instrumental Analysis*, 6th ed.; Thomas Brooks/Cole: California, 2007.
10. Aslan, K.; Geddes, C. D.; *Chem. Soc. Rev.*, **2009**, 38, 2556 – 2564.
11. Geddes, C.D.; Cao, H.; Gryczynski, I.; Gryczynski, Z.; Fang, J.; and Lakowicz, J.R.; *J. Phys. Chem. A*, **2003**, 107, 3443-3449.

MANUSCRIPT 1

To be submitted to Applied Spectroscopy, **2013**

Fabrication of SERS Substrates for Explosive Testing

Meredith A. Matoian, Emily C. Hall, Courtney McGowan, William B. Euler*

Corresponding Author:

Prof. William B. Euler

Department of Chemistry

University of Rhode Island

Kingston, RI 02881

weuler@chm.uri.edu

Manuscript 1

Fabrication of SERS Substrates for Explosive Detection

Abstract

Surface Enhanced Raman Scattering (SERS) active substrates were created through the redox reaction of freshly etched porous Silicon (p-Si) and aqueous AgNO_3 . The result was a porous silicon substrate coated with a layer of silver nanoparticles with an approximate thickness of 200 nm as estimated by AFM and XPS. The substrate shows promising results for the detection of explosives, namely trinitrotoluene (TNT), dinitrotoluenes (2,3-DNT, 2,4-DNT, 2,6-DNT, 3,4-DNT), and cyclotrimethylenetrinitramine (RDX).

Introduction

In the recent years, great advances in the area of detection have been made, specifically in Surface Enhanced Raman Scattering (SERS). SERS is a technique that utilizes the surface plasmon resonance of metal nanoparticles to amplify signals that contain vibrational information of the analyte. While single molecule detection has been reported, this sort of response is not typical. Rather, signal enhancements on the order of 10^3 - 10^6 are more commonly reported.^{1,2} Even at this level, trace detection is possible and far exceeds the response seen by traditional Raman, with typically diminished fluorescence interference.¹ Unfortunately, creating SERS-active substrates for varying applications can be challenging, with many steps of optimization.

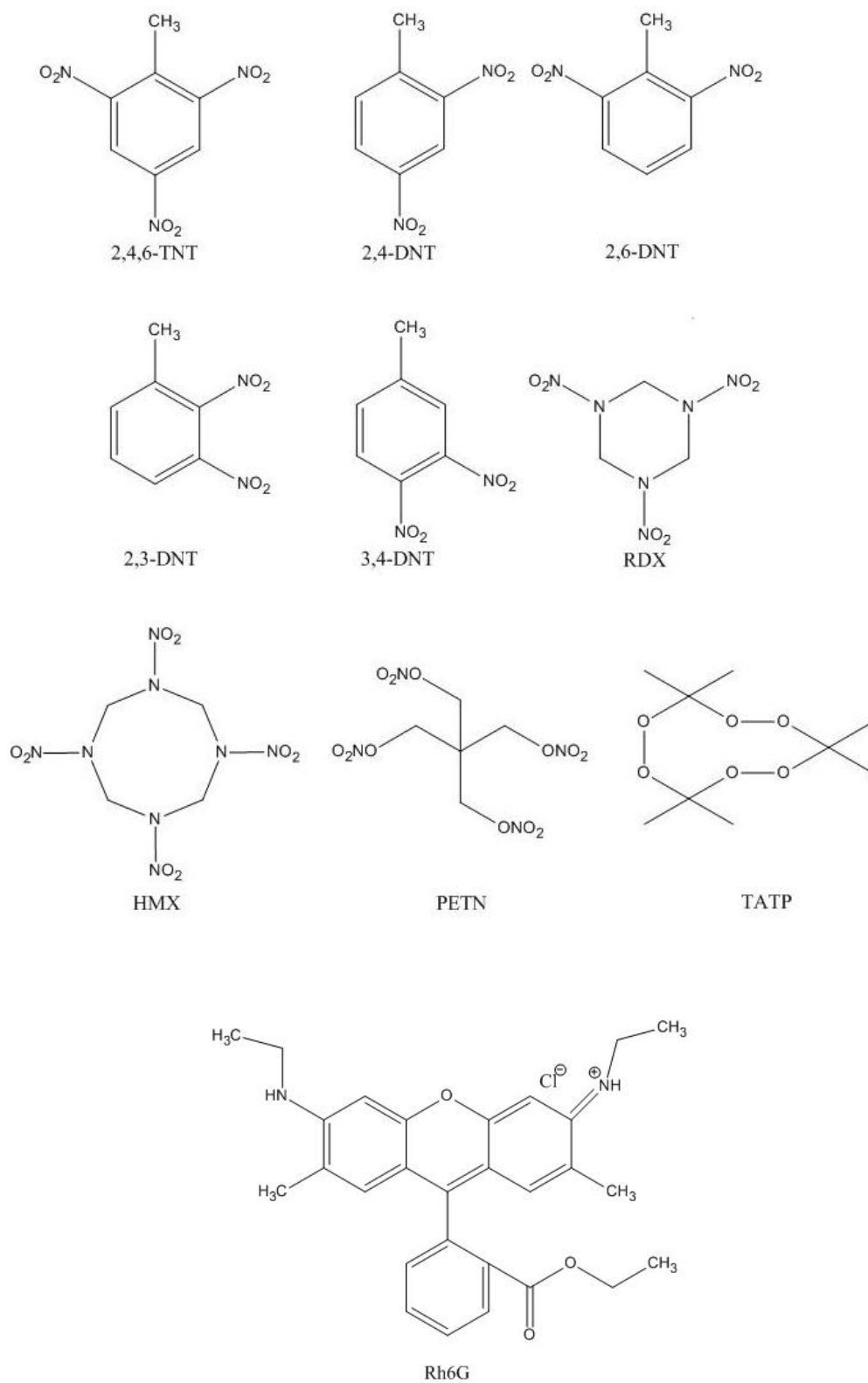
Growing steadily with the improvements in detection has been the number of terrorist attacks, both at home and abroad, and the use of explosive materials in these actions. These materials have proven to be difficult to detect by a standoff detection method because of their extremely low vapor pressures, making research in the area important. This research group has worked closely with EmiTech, Inc. to optimize a novel explosive sensor, known as Mark I.³ The sensor operates by combining the increased surface area of porous silicon with a conjugated fluorescent polymer that is known to quench in the presence of nitroaromatic explosives. Specifically, the sensor has shown to be sensitive to the vapors of trinitrotoluene (TNT), cyclotrimethylenetrinitramine (RDX), and pentaerythritol tetranitrate (PETN) (Scheme 1). The following research discusses the work that has been done independently to improve upon the concept of the existing sensor by adding a SERS-active substrate to increase selectivity. As many chemical vapors are known to cause fluorescent quenches, the added vibrational mode information could limit the number of false positives and potentially identify respective explosives, allowing for a detailed plan of action to be created by response personnel.

Raman and SERS detection of explosives has been reported in a variety of research approaches. In 2000, Sylvia et al.⁴ were able to detect 2,4-dinitrotoluene (2,4-DNT) (Scheme 1), a known impurity in TNT, as low as 5 ppb for landmine identification. The SERS-active substrate were roughened Au and required a 0.01 M NaOH mist to show the significant enhancement in the spectrum of 2,4-DNT.⁴ Jerez-Rozo et al.¹ in 2008 utilized metal colloids for SERS detection of TNT. SERS spectra of 1×10^{-10} g of TNT solutions were obtained on Ag, Au, and Au/Ag colloids with

enhancement factors on the order of 10^{11} .¹ More recently, Ehlerding et al.⁵ has attempted resonance-enhanced Raman spectroscopy on 2,4-DNT and TNT vapors. Solid samples of the explosives were heated to achieve 1445 ppm 2,4-DNT and 341 ppm TNT concentration for detection.⁵ To achieve enhancements on the order of 10^4 – 10^5 the incident light was changed from 532 nm to 232 nm.⁵ This approach also proved to be applicable to the standoff detection, making it an attractive option for research and a possible direction for future work for this research group. The other two previous research approaches, while successful in the detection of explosives, require complicated sample preparation and numerous steps of optimization. The concept of immersion plating on p-Si provided a simpler production of a SERS-active substrate. Using this technique, a substrate made through easy and cost-effective techniques with promising results has been developed.

Experimental Section

Chemicals. Hydrofluoric acid 49% was obtained from Fisher Scientific. Absolute ethanol (99.9% from Pharmco-Aaper) and 18.2 M Ω water were used to dilute the HF and create the etching solution. AgNO₃ (Sigma-Aldrich, $\geq 99.0\%$) solutions for Ag deposition were created in 18.2 M Ω water. Raman studies were completed with Rhodamine 6G (Rh6G) (Acros Organics) and explosive compounds (Drs. Oxley and Smith, URI) including TNT, dinitrotoluenes (2,3-DNT, 2,4-DNT, 2,6-DNT, 3,4-DNT), RDX, cyclotetramethylenetetranitramine (HMX), pentaerythritol tetranitrate (PETN), and triacetone triperoxide (TATP). Structures can be seen in scheme 1.



Scheme 1. Analytes utilized for Raman studies.

Silicon Wafers. Polished p-type, B-doped silicon wafers <100> with resistivity 0.01 – 0.02 Ωcm and thickness of 500 – 550 μm were purchased from Silicon Quest International.

Electrochemical Etching. Flat silicon wafers are first cut down to a 4 cm by 4 cm size and mounted in the Teflon etching chamber equipped with a copper electrode and a platinum mesh electrode. An aqueous HF solution (1:1:0.9 H_2O : EtOH: HF) is poured over the wafer immediately before current is applied. Constant current is applied by a Keithley 2635A SYSTEM sourcemeter with accompanying software. All samples were prepared with a current of 25 mA/cm^2 for 190 seconds.^{6,7}

Silver Deposition. Freshly etched p-Si samples were cut down to 4 cm^2 in size and immersed in 50 mM AgNO_3 . The p-Si/Ag samples were then rinsed with water and dried by $\text{N}_2(\text{g})$.⁸⁻¹⁰

Raman Measurements. An Agiltron PeakSeeker Raman spectrometer was used to collect Raman spectra. The excitation source was a diode laser at 785 nm. Rh6G and the explosive analytes were usually dissolved in ethanol to create concentrations ranging from 1.0×10^{-3} to 1.0×10^{-5} M solutions. A respective solution was selected to be applied to the sensor substrates in a typical volume of 30 μL and allowed to dry in air before spectra were obtained. Surface concentration was calculated in moles per centimeter² using the concentration, volume, and average area of a substrate (3.47 cm^2). Three to five spots on the sensor for detection were chosen randomly.

Atomic Force Microscopy Images. Images were collected on an Agilent 5500 AFM in tapping mode. The cantilevers were purchased from Nanosensors and had a force constant of 10-130 N/m. Prior to acquiring data, a calibration grid with a step height of 104 nm was imaged.

X-ray Photoelectron Spectroscopy (XPS). Spectra were collected on a PHI 5500 instrument through the Sensor and Surface Technology Partnership at the University of Rhode Island.

Results and Discussion

Coating of the p-Si samples with a roughened Ag layer by immersion plating has been studied and reported previously.⁸⁻¹⁰ The spontaneous deposition of Ag by the reduction of Ag^+ occurs due to the mild reducing power of the freshly etched p-Si. The p-Si surface, made of Si-H bonds, is oxidized to SiO_2 . Noted for being cheap in cost and easy in preparation, the technique was selected for this study. As the morphology of the Ag surface is dependent on the substrate structure and the conditions of deposition, such as length of time and concentration of AgNO_3 , preliminary studies were needed to create the optimal SERS-active substrate. As discussed previously, etching procedures were already known to this research group, meaning the substrate structure was already determined.^{6,7} Additionally, Zieri *et al* had found that an aqueous 50 mM AgNO_3 solution provided the largest SERS

enhancement of the Rh6G spectrum⁸, leaving only the length of time for the Ag deposition to be determined.

Samples were produced following the procedure outlined above with varying Ag-deposition times to determine the appropriate length of growth for the porous silicon substrates. Rh6G was selected for this study due to its known high Raman cross section.¹¹ Figure 1 shows a sample of the spectra collected from 4.3×10^{-10} mol/cm² Rh6G on p-Si/Ag substrates. Growth times included 0, 10, 12, 14, 16, 18, 20, and 22 minutes. While the 12 minute deposition appears to have the highest intensity at the characteristic Rh6G peaks, the height difference can be attributed to the increased baseline. Figure 1 was created with the “hot spot,” or best result, of Rh6G on each growth time. As the sample is not completely uniform, it is possible that all acquired spectra taken at varying locations could produce only a fraction of the potential enhancement. Taking this fact into consideration, Figure 2, which represents the average intensity at the 1517 cm⁻¹ Rh6G peak over three scans, was created for the determination of deposition time. On average, the 14 minute Ag deposition provided the most intense Rh6G spectrum. It is also important to observe that the 0 minute Ag growth, indicating only p-Si, showed no Rh6G spectrum, justifying that the Ag layer is responsible for the enhancement. All SERS substrates generated after this study and for the remainder of this paper were created with the length of Ag growth parameter held constant at 14 minutes.

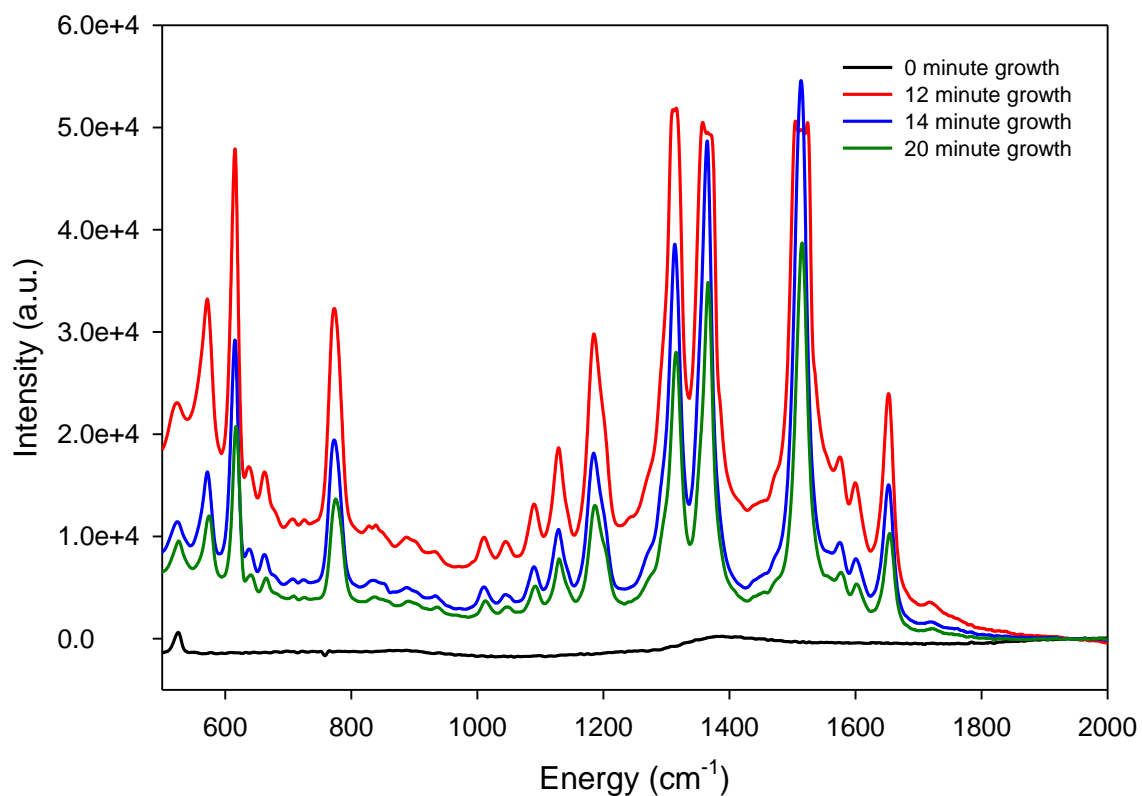


Figure 1. Raman spectra of Rh6G on p-Si/Ag substrates with varying length of Ag growth. All samples were etched in the same fashion and 40 μL of 3.7×10^{-5} M Rh6G solution was deposited (4.3×10^{-10} mol/cm² Rh6G). Spectra were baseline corrected at 1939 cm⁻¹.

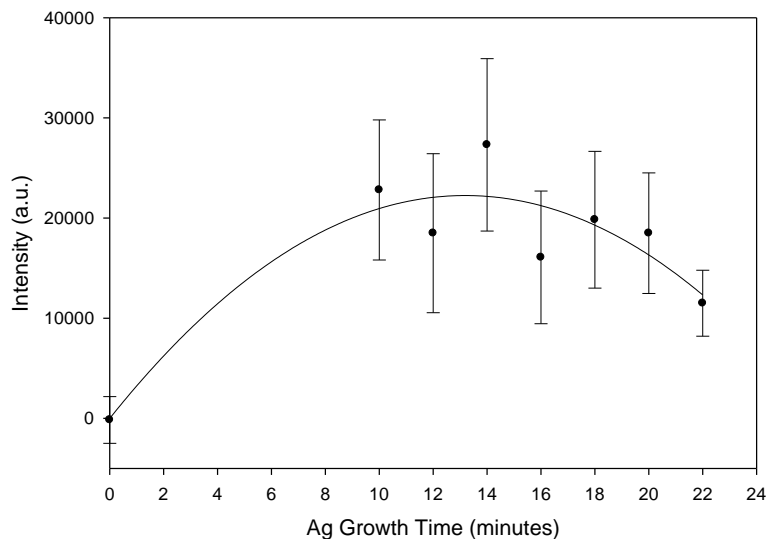


Figure 2. The average Raman intensity of 4.3×10^{-10} mol/cm² Rh6G at 1517 cm⁻¹ was plotted versus Ag growth time. Each Ag deposition time had at least three replicate samples, with three spectra collected from each. Data were baseline corrected at 1939 cm⁻¹ previous to determining average intensity.

The resulting Ag layer is approximately 200 nm thick, as demonstrated by the AFM image in Figure 3. As shown by the image, thickness of the Ag layer varies across the sample. While features with heights of approximately 700 nm are shown, features of 200 nm height are more prevalent. This is supported by the calculated roughness, or root mean square height, of 135 nm. Additional height information can be found in supplementary material Table 1. The suspected Ag features are the light blue/green islands, which reside approximately 700 nm apart. It is suspected that the dark blue areas are the p-Si substrate. Whether these areas are pores or the tops of the Si spires is unknown. X-ray photoelectron spectroscopy (XPS) was completed for additional information in this area.

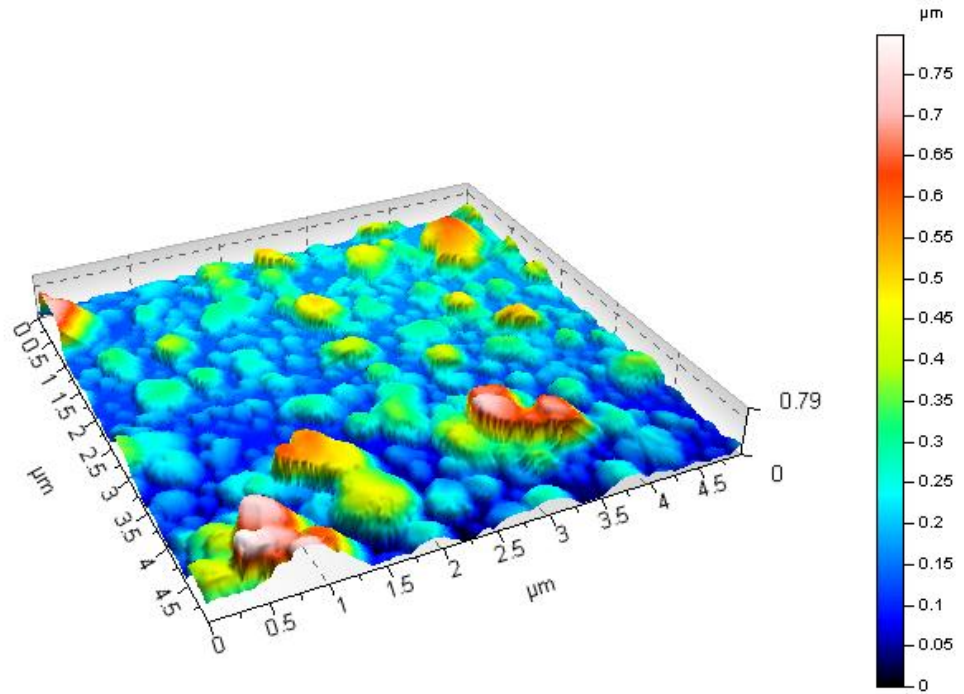


Figure 3. AFM image of a 5 μm by 5 μm region of a p-Si/Ag substrate.

XPS was utilized to better understand the characteristics of the Ag layer and for further clarification of the AFM image. Figure 4 shows both the full spectrum (A) and the Si region (B). The results seen in Figure 4A show strong Ag signals and minor Si signals. Figure 4B is a magnified portion representing only the bonding energies associated with Si. Noting the poor signal to noise and knowing the penetration depth of XPS is between 1 and 10 nm, it can be again concluded that the thickness of the Ag layer varies. Therefore, the generated surface is best described as a roughened Ag surface.

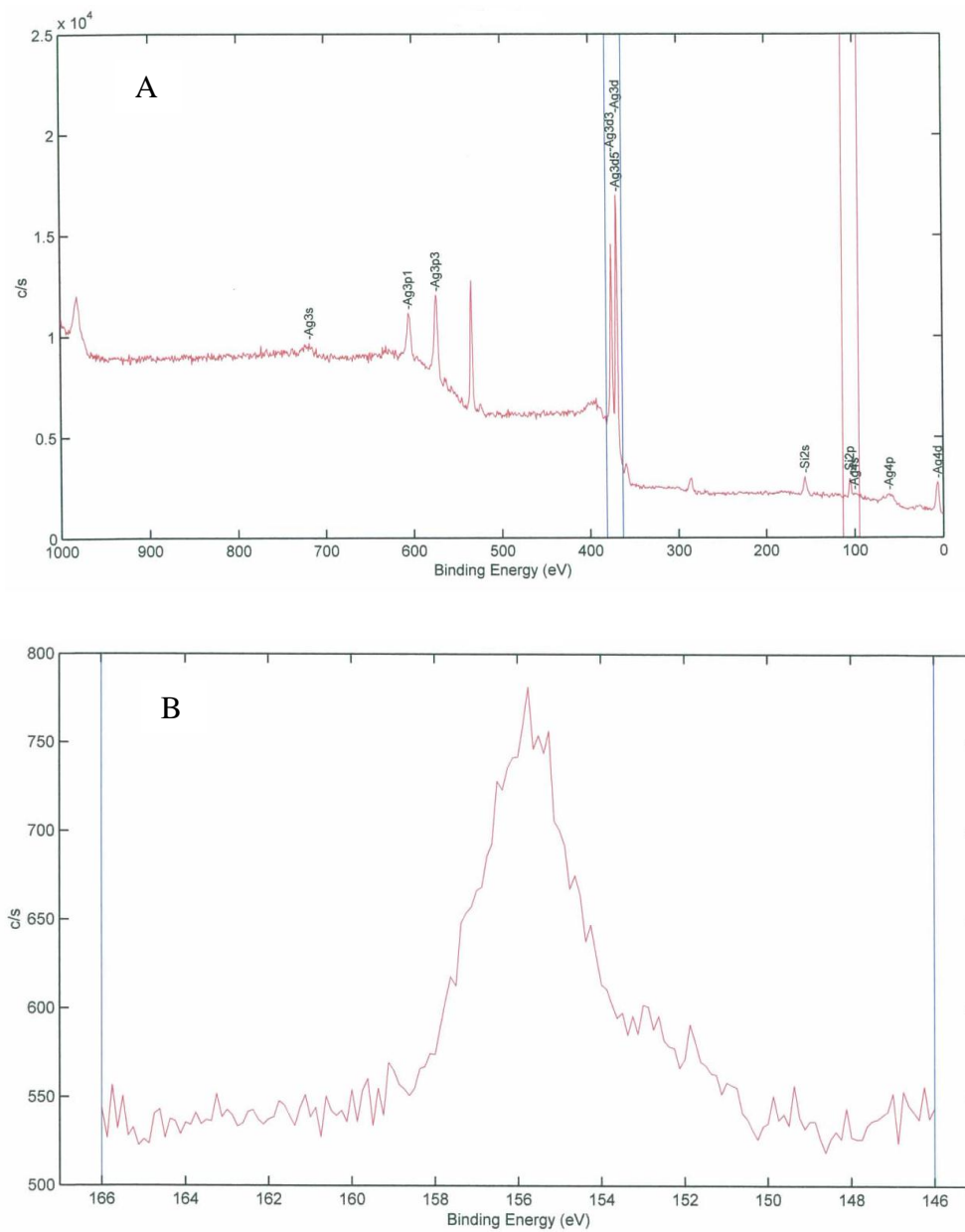


Figure 4. XPS data collected from a p-Si/Ag sample. A) Full spectrum B) Si spectra showing poor signal to noise. Major peaks are labeled with the appropriate species. The unlabeled peaks on the full spectrum correspond to oxygen, nitrogen and carbon.

A study to approximate the limit of detection for the Raman active substrates on the Agilitron instrument was completed, once again utilizing Rh6G. Even with an average Raman instrument, detection of Rh6G was possible in the 10^{-9} mol/cm² range (Figure 5). While the drop in intensity from 3.5×10^{-9} mol/cm² to 1.2×10^{-9} mol/cm² is abrupt as seen in Figure 6, typical Rh6G peaks can still be observed in the lowest concentration when multiplied by a factor of 50. This concentration represents the approximate limit of the instrument's capabilities. The experiment provided a starting point for further work with other solutions of interest.

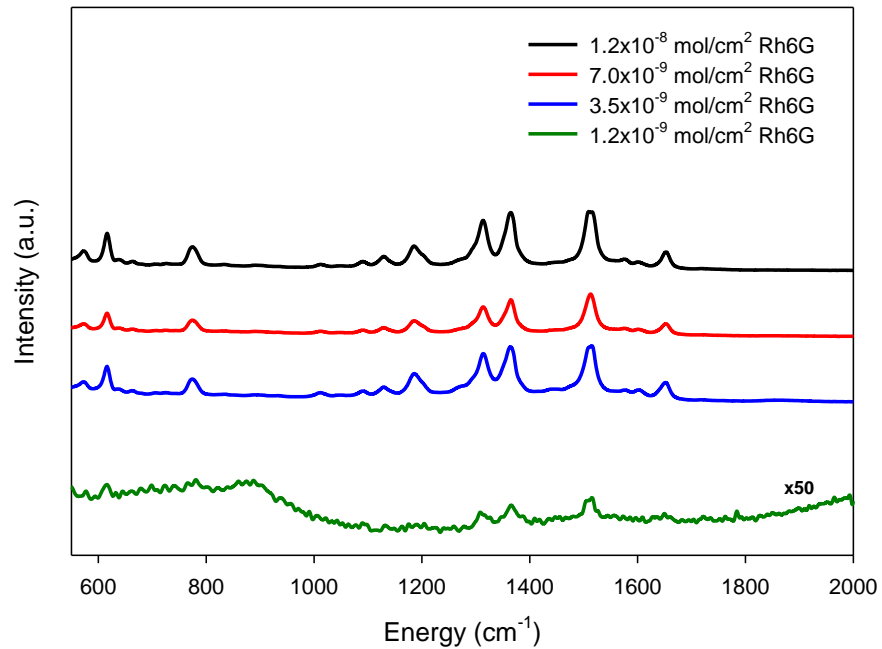


Figure 5. Raman spectra obtained of Rh6G on p-Si/Ag substrates used to determine the limit of detection of the Agilitron instrument.

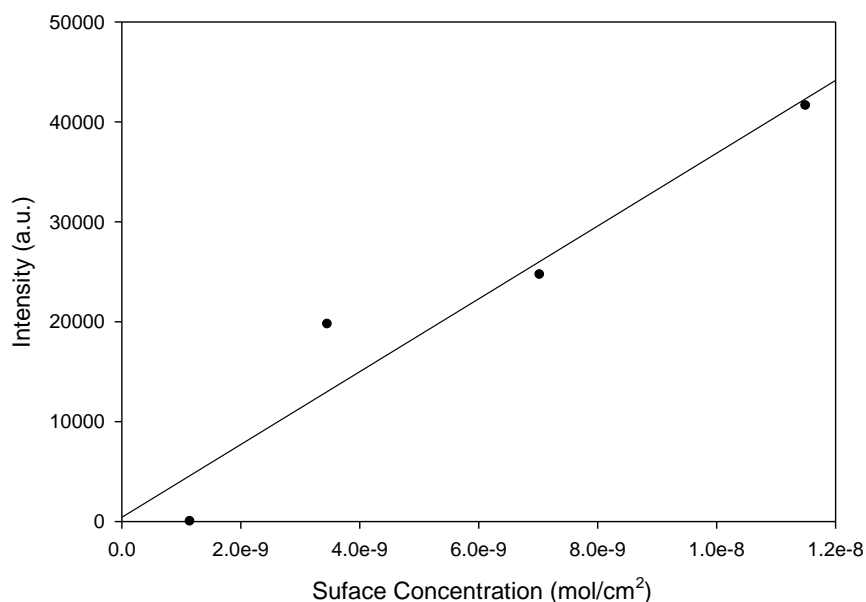


Figure 6. Raman intensity obtained of Rh6G at 1517 cm^{-1} on p-Si/Ag substrates used to determine the limit of detection of the Agilitron instrument. Intensities were background corrected at 2138 cm^{-1} .

To show that SERS detection of explosives is possible, $30\text{ }\mu\text{L}$ of a respective explosive analyte was applied directly to p-Si/Ag substrates as a proof of concept. The ethanolic solutions were all approximately 10^{-4} M and gave minimal, but visible, responses. Figure 7 shows the SERS spectra of RDX (A), 2,4,6-TNT (B), 2,4-DNT (C), 2,6-DNT (D), 2,3-DNT (E), and 3,4-DNT (F). Spectra of HMX, PETN, and TATP were also attempted, but no distinct peaks were observed at the investigated concentrations. These preliminary results verify that explosives produce a unique fingerprint that can be used to identify specific bonds present in the molecule of interest. Major peaks visible in the Raman spectra were assigned in Table 1. The peak at 1600 cm^{-1} , for example, can be assigned to the vibrations of the aromatic

carbon-carbon bonds in TNT and the DNTs. As RDX does not share this common feature, no peak corresponding to this vibration was seen. Only a single peak that corresponds to the vibrations of the nitrogen-nitrogen bonds was visible for RDX. Again, as this feature is unique to RDX in the set of selected analytes, the feature at 1073 cm^{-1} was not visible in the other spectra. While peaks may be shared between common molecules, the overall spectra show specificity depending on substitutions and structural changes. With further optimization of the SERS substrate, vapor testing may be possible.

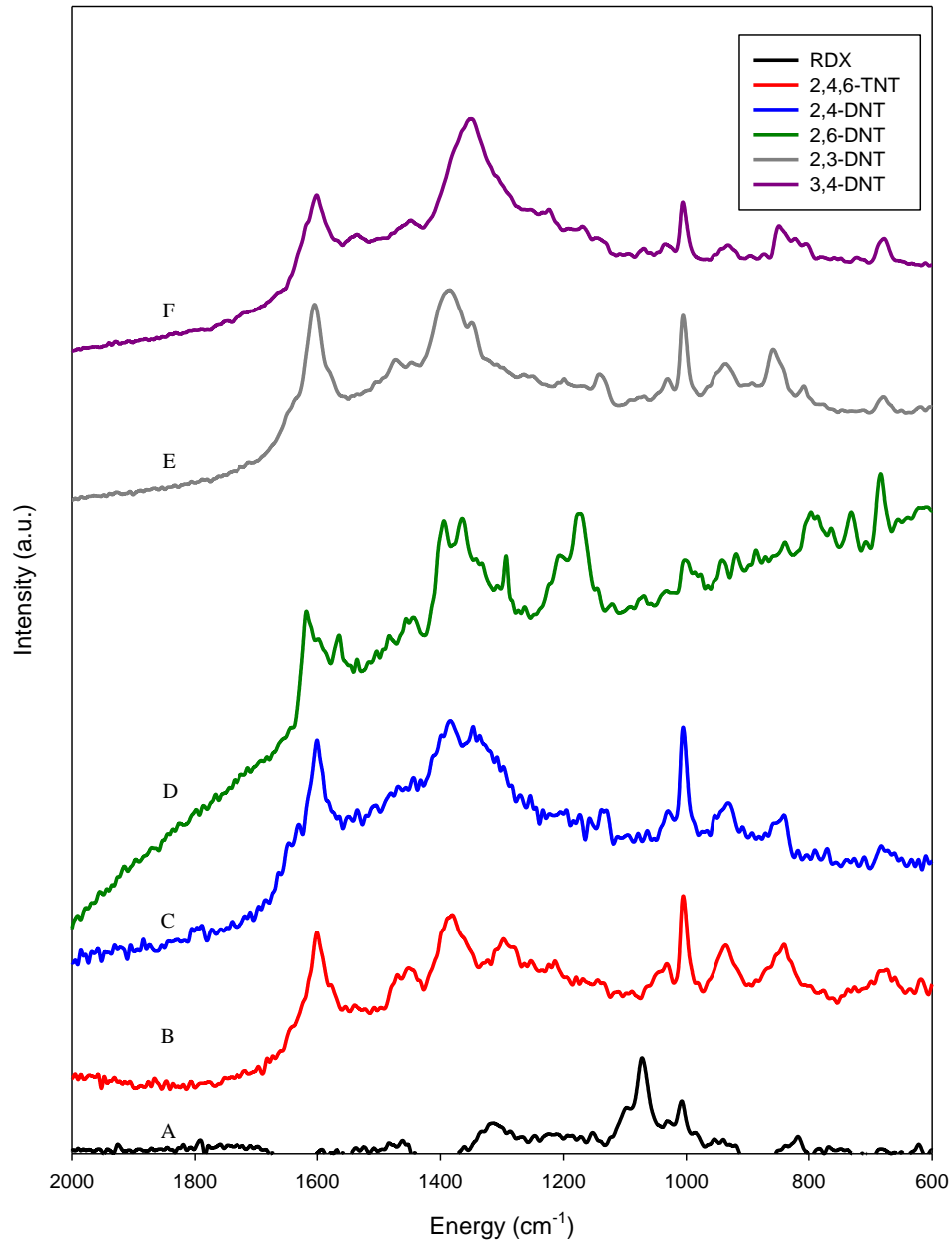


Figure 7. SERS spectra of explosive analytes on p-Si/Ag substrates. The spectra are baseline corrected at 1704 cm^{-1} and adjusted in intensity for clarification of the peaks. A) $1.4 \times 10^{-9}\text{ mol/cm}^2$ RDX; B) $9 \times 10^{-10}\text{ mol/cm}^2$ TNT; C) $1.3 \times 10^{-9}\text{ mol/cm}^2$ 2,4-DNT; D) $1.3 \times 10^{-9}\text{ mol/cm}^2$ 2,6-DNT; E) $1.3 \times 10^{-9}\text{ mol/cm}^2$ 2,3-DNT; F) $1.3 \times 10^{-9}\text{ mol/cm}^2$ 3,4-DNT.

| Wavenumber (cm ⁻¹) | | | | | | Band Assignment |
|--------------------------------|---------|---------|-----------|-----------|------|--|
| 2,4,6-TNT | 2,4-DNT | 2,6-DNT | 2,3-DNT | 3,4-DNT | RDX | |
| 1600 | 1600 | 1618 | 1605 | 1600 | - | ν (CC) aromatic ring chain vibration |
| 1550 (sh) | - | 1535 | 1550 (sh) | 1545 (sh) | - | ν (C-(NO ₂)) asymmetric |
| 1418 | - | 1423 | 1442 | 1423 | - | δ (CH ₃) asymmetric |
| 1370 | 1346 | 1356 | 1370 | 1341 | - | ν (C-NO ₂) symmetric |
| 1002 | 1002 | 996 | 1007 | 1007 | - | ν (CC) aromatic ring chain vibration |
| - | - | - | - | - | 1073 | ν (N-N) |

Table 1. Raman peaks for each analyte assigned to a specific structural feature, where “sh” represents shoulder. The resolution of the instrument is 4 cm⁻¹.

Conclusions

Through experimental work, a SERS-active substrate was created and optimized for the established etching procedure. It was found that a 14 minute Ag deposition results in the largest enhancement of Rh6G. Rh6G also was utilized to determine a limit of detection of the Agilent instrument with the p-Si/Ag substrates. The Raman spectrometer was able to detect down to the 10⁻⁹ mol/cm² level, providing a starting point for solution explosive testing. Finally, these substrates show that explosive detection is possible and with further optimization vapor phase explosive detection may be achieved.

References

1. Jerez-Rozo, J.I.; Primera-Pedrozo, O.M.; Barreto, Cabán, M.A.; Hernández-Rivera, S.P.; *IEEE Sens. J.*, **2008**, 8, 974 – 982.
2. Skoog, D.A.; Holler, F.J.; Crouch, S.R.; *Principles of Instrumental Analysis*, 6th ed.; Thomas Brooks/Cole: California, 2007.
3. http://www.emitechinc.com/chem_nanosensors.html (accessed Nov. 1, 2012).
4. Sylvia, J.M.; Janni, J.A.; Klein, J.D.; and Spencer, K.M.; *Anal. Chem.*, **2000**, 72, 5834 - 5840.
5. Ehlerding, A.; Johansson, I.; Wallin, S.; and Östmark, H.; *International Journal of Spectroscopy*, **2012**, 2012.
6. Levitsky, I. A.; Euler, W. B.; Tokranova, N.; and Rose, A.; *Appl. Phys. Lett.*, **2007**, 90, 041904/1 – 041904/3.
7. Brodeur, D.R. Ph.D. Dissertation, University of Rhode Island, 2011.
8. Zeiri, L.; Rechav, K.; Porat, Z.; Zeiri, Y.; *Appl. Spec.*, **2012**, 66, 294 – 299.
9. Chursanova, M.V.; Germash, L.P.; Yukhymchuk, V.O.; Dzhagan, V.M.; Khodasevich, I.A.; Cojoc, D.; *Appl. Surf. Sci.*, **2010**, 256, 3369 – 3373.
10. Harraz, F.A.; Tsuboi, T.; Sasano, J.; Sakka, T.; and Ogata, Y.H.; *J. Electrochem. Soc.*, **2002**, 149, C456 – C463.
11. Mullin, J.; Schatz, G.C.; *J. Phys. Chem. A.*, **2012**, 116, 1931 – 1938.

Supplementary Information

| Height Parameters | | | |
|-------------------|--------|---------------|--------------------------------|
| Sq | 0.135 | μm | <i>Root mean square height</i> |
| Sp | 0.554 | μm | <i>Maximum peak height</i> |
| Sv | 0.244 | μm | <i>Maximum pit height</i> |
| Sz | 0.798 | μm | <i>Maximum height</i> |
| Sa | 0.0988 | μm | <i>Arithmetic mean height</i> |

Table 1. Further height parameters for the AFM image of the p-Si/Ag sample seen in

Figure 3.

MANUSCRIPT 2

To be submitted the Journal of Fluorescence, **2013**

Light Trapping to Amplify Metal Enhanced Fluorescence with Application for
Sensing TNT

Meredith A. Matoian, Richard Sweetman, Emily C. Hall, Shayna Albanese, William
B. Euler*

Corresponding Author:

Prof. William B. Euler

Department of Chemistry

University of Rhode Island

Kingston, RI 02881

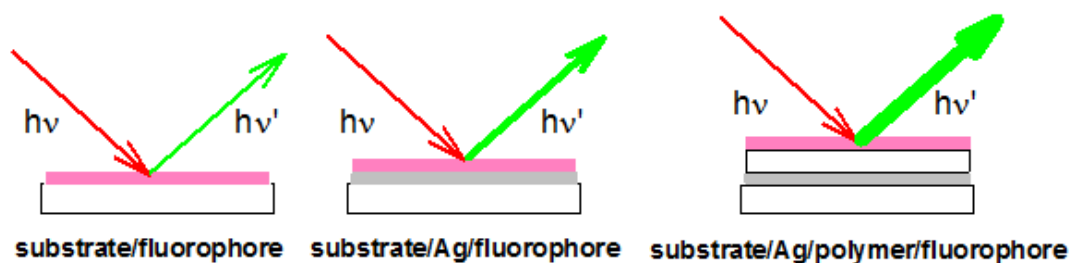
weuler@chm.uri.edu

Manuscript 2

Light Trapping to Amplify Metal Enhanced Fluorescence with Application for Sensing TNT

Abstract

Metal Enhanced Fluorescence (MEF) typically produces enhancement factors of 10 to 50. By using a polymer layer as the dielectric spacer enhancements as high as 1600 can be observed. The effect occurs with a variety of different polymers and substrates. This allows the fabrication of sensors with improved sensitivity as demonstrated for detection of trinitrotoluene (TNT).



Scheme 1. Varying substrate assemblies utilized in this study to demonstrate the enhancement of fluorescent emission.

Introduction

Exploitation of the plasmon properties of metal nanoparticles is currently of interest. Coupling the electric field created by a plasmon to a molecule on the surface can lead to significant intensity increases in Raman spectra (surface enhanced Raman spectra, SERS) and in fluorescent spectra (metal enhanced fluorescence spectra, MEF).¹⁻⁸ For SERS, typical enhancements can be 10^6 or greater while for MEF the

enhancements are more modest, typically $10^1 - 10^2$. We have been interested in using fluorescence methods for the detection of explosives.⁹ A porous silicon (p-Si) substrate is used as the substrate for the fluorophore, which increases the surface area available to the analyte, thereby increasing the sensitivity. We presumed that adding a metal layer to the porous layer the sensitivity could be further improved by taking advantage of MEF. Optimized MEF structures require a dielectric layer between the metal and the fluorophore and when we used a polymer as the dielectric the enhancements increased to $10^2 - 10^3$.

We report here that using a polymer layer between a fluorophore and substrate provides an enhanced emission for a variety of polymers and substrates, including those that do not include a metal layer. The enhancement appears to arise from a combination of effects since a single mechanism does not account for the observed intensities. When the substrate contains a layer of silver nanoparticles the MEF effect is amplified cooperatively by the polymer effect. We exploit this effect to demonstrate improved sensitivity for the detection of trinitrotoluene (TNT).

Experimental Section

Silver coated porous silicon substrates, p-Si/Ag, were created by electrochemical etching⁹ and reduction of silver nitrate solution on the freshly etched pores.¹⁰ Flat silicon wafers (p-type <100>, Silicon Quest International) are first cut down to a 4 cm by 4 cm size and mounted in a Teflon etching chamber. An aqueous HF solution (100:100:90 v/v H₂O: EtOH: HF) was poured over the wafer immediately before current is applied. Constant current was applied by a Keithley 2635A

SYSTEM sourcemeter using 25 mA/cm^2 current for 190 seconds. The resulting p-Si has pores with approximately 10 micron diameter.⁹ Freshly etched p-Si samples were then submerged in a 50 mM AgNO_3 solution for 14 min. A chosen polymer was spin-cast on the p-Si/Ag wafer at a rate of 1200 rpm for 45 seconds (acceleration rate 1296 /s/s), followed by drying in a 60 °C oven for 2 min to evaporate residual solvent. Polymer solutions used were 2 % w/v poly(vinylidene fluoride), PVDF, in 90/10 (v/v) acetone/dimethyl formamide (DMF) mixture, 3 % w/v $[(\text{CH}_2\text{CF}_2)_{0.65}(\text{CHF}\text{CF}_2)_{0.35}]_x$, co-polymer, in acetone/DMF, and 5 % w/v polymethylmethacrylate, PMMA, in tetrahydrofuran (THF). 30 μL of the selected fluorophore (6.0×10^{-4} M of rhodamine 6G, Rh6G, or 6.5×10^{-4} M methoxy-ethylhexyloxypolyphenylene-vinylene, MEH-PPV), was applied to the p-Si/Ag/polymer samples and allowed to dry in air to complete the MEF substrates. The average area of the sample was 3.5 cm^2 ; using the densities of the fluorophores this gave an estimated thickness of 20 nm for Rh6G and 40 nm for MEH-PPV. Substrates were mounted on glass slides to fit the solid sample holder for the Horiba Fluorolog-3 instrument, for fluorescence measurements. The incidence angle was set to 55° from perpendicular, which was determined to provide the maximum response. For all measurements reported here, the slit width was set to 1 nm for both the excitation and emission monochromators. Reflection spectra were obtained using an Ocean Optics spectrometer with a reflectance probe at 90° incidence from the sample.

Results and Discussion

Figure 1 shows the emission spectra for rhodamine 6G (Rh6G) on several different substrates. When Rh6G is placed directly on p-Si a weak luminescence is observed with a maximum at 555 nm. When a layer of Ag nanoparticles (~100 – 200 nm thick islands, as estimated by AFM) is placed between the fluorophore and the p-Si the emission intensity increases by a factor of 3, which is typical for MEF with no dielectric layer. Using a transparent polymer as the dielectric spacer, giving a structure of p-Si/Ag/polymer/Rh6G, leads to dramatic enhancements, as shown in Fig. 1 (the spectra are normalized to the maximum of the p-Si/Rh6G sample so the ordinate represents the enhancement factor). These are significantly increased compared to what is usually observed in MEF and are especially unusual since the polymer layers are ~10 – 20 times thicker than the usual dielectric layers used in MEF structures. There are also shifts of the wavelength maximum that are not typically seen in MEF.

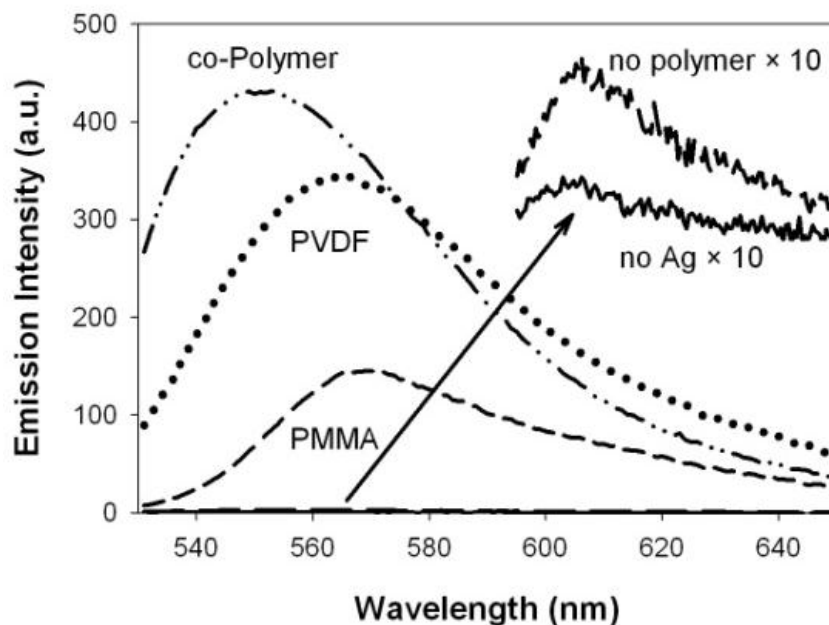


Figure 1. Emission spectra of Rhodamine 6G coated on different polymers cast on a porous Si/Ag substrate. All spectra are normalized to the spectrum with no Ag and no polymer, p-Si/Rh6G (solid line). MEF samples were: no polymer, p-Si/Ag/Rh6G (long dashed); p-Si/Ag/PMMA/Rh6G (short dashes); p-Si/Ag/PVDF/Rh6G (dotted); and p-Si/Ag/co-Polymer/Rh6G (dot-dashed). The inset shows the p-Si/Rh6G and p-Si/Ag/Rh6G spectra multiplied by 10. Excitation was at 521 nm and 1 nm slits were used for both the excitation and emission monochromator.

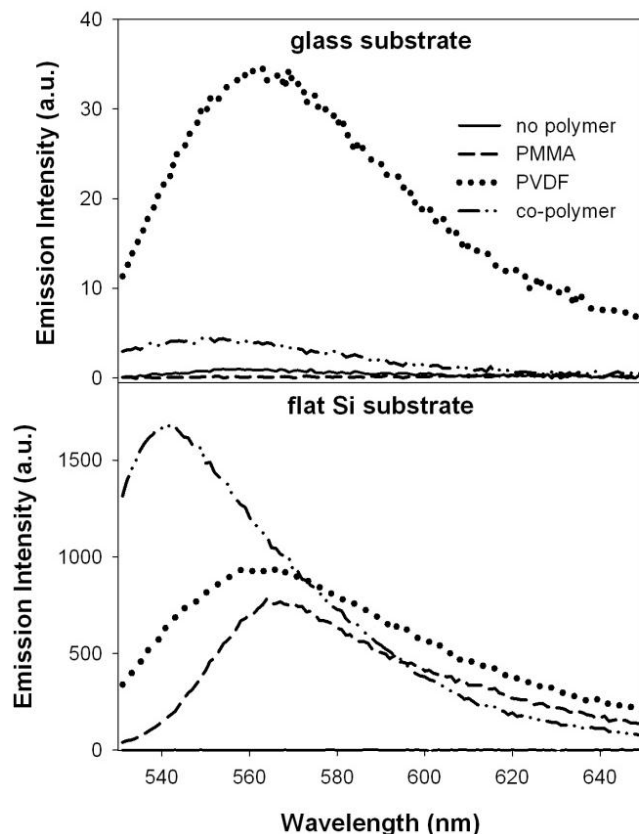


Figure 2. Emission spectra of Rhodamine 6G coated on different polymers cast on a glass substrate (upper) and a flat Si substrate (lower). All spectra are normalized to the spectrum with no polymer (solid line). PMMA (short dashes), PVDF (dotted), and co-Polymer (dot-dashed). Excitation was at 521 nm and 1 nm slits were used for both the excitation and emission monochromator.

To test the effect of different substrates, Rh6G was deposited onto polymers spin-cast onto a glass slide and a flat Si wafer. Neither of these substrates contained Ag, yet substantial enhancements were observed as shown in Figure 2. Even with a glass slide substrate there is a modest enhancement, by as much as a factor of ~35 for PVDF. When the substrate is flat Si, again with no Ag, the polymers lead to enormous enhancements, as high as 1600 for 0.3 μm thick co-polymer film. On the flat Si

substrate there also is noticeable shift of the emission maximum, with maxima ranging from 560 nm for PMMA, 550 nm for PVDF, and 540 nm for the co-polymer. When Fabry-Perot modes are coupled to a plasmon resonance the absorption maximum can shift¹¹ and this should affect the emission maximum similarly. However, the flat Si is a semiconductor and is not expected to support a plasmon resonance. There is a considerable difference in the polarity of each of these polymers and that may contribute to the observed wavelength shift.

Figure 3 shows the emission spectra for different substrates all spin-cast with a $\sim 0.3 \mu\text{m}$ PVDF film, normalized to Rh6G on glass with no polymer. When the substrate is glass, flat Si, or p-Si the enhancements are all comparable, ~ 400 , relative to the glass substrates, glass/Rh6G. The enhancement more than doubles when Ag is deposited on the p-Si. This shows that the plasmon induced enhancement and the polymer amplification are cooperative and multiplicative.

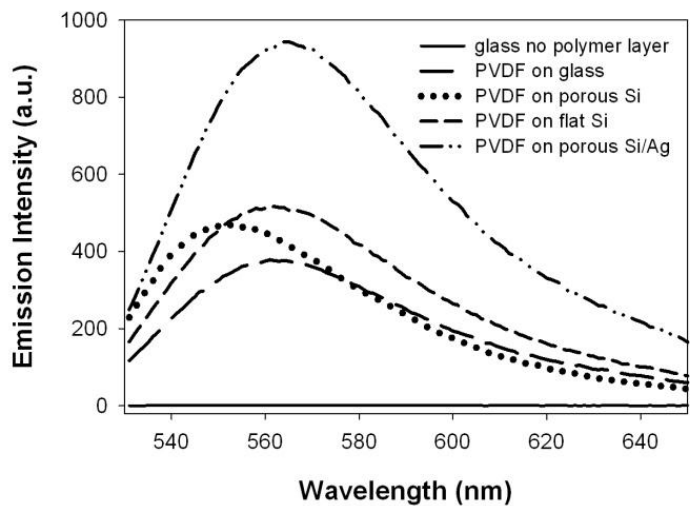


Figure 3. Emission spectra of Rhodamine 6G cast on PVDF with different substrates. All spectra are normalized to Rhodamine 6G cast on glass with no polymer layer (solid line). PVDF on glass (long dashes), PVDF on porous Si (dots), PVDF on flat Si (short dashes), PVDF on Ag coated porous Si (dot-dashed line). Excitation was at 521 nm and 1 nm slits were used for both the excitation and emission monochromator.

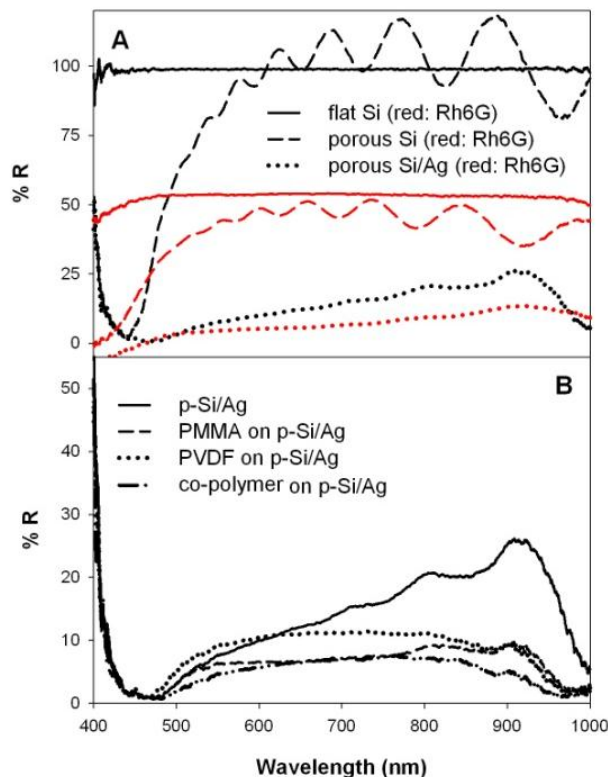


Figure 4. A. Reflection spectra of flat Si substrate (black solid line), flat Si substrate coated with Rhodamine 6G (red solid line), porous Si substrate (black dashed line), porous Si substrate coated with Rhodamine 6 (red dashed line), Ag coated porous Si (black dotted line), and Ag coated porous Si substrate coated with Rhodamine 6G (red dotted line). B. Reflection spectra of Ag coated porous Si (solid line), ~310 nm PMMA on Ag/p-Si (dashed line), ~470 nm PVDF on Ag/p-Si (dotted line), and ~150 nm $[(\text{CH}_2\text{CF}_2)_{0.65}(\text{CHF}\text{CF}_2)_{0.35}]_x$ co-polymer on Ag/p-Si.

Reflection spectra for the various structures were measured, as shown in Figure 4. The effect of simply depositing Rh6G onto the substrate is shown in Fig. 4A using flat Si as the reference. In the absence of Rh6G, p-Si shows a fringing pattern resulting from the pore structure ($\sim 2 \mu\text{m}$ thick) but the fringing largely disappears

when the Ag layer is added, indicating that the light does not pass through to the p-Si layer. The p-Si shows a resonance at 450 nm while the p-Si/Ag substrate shows minimal reflection throughout the visible region. Upon addition of Rh6G, reflection drops considerably in all cases and does not show any feature that could be assigned to the absorption maximum expected for Rh6G at 521 nm. The featureless response indicates that the Rh6G layer is trapping light. Fig. 4B shows the reflection spectra of different polymers, with no Rh6G, coated onto p-Si/Ag. The polymers, which are all transparent, all reduce the reflectivity compared to the bare p-Si/Ag, showing that the polymers also trap the light within the structure.

Samples were prepared using MEH-PPV on flat Si and p-Si/Ag/co-polymer substrates to be used for TNT sensing. MEH-PPV has been previously shown to be effectively quenched by nitroaromatics.⁹ As expected, the p-Si/Ag/co-polymer/MEH-PPV structure showed a fluorescence enhancement compared to flat-Si/MEH-PPV, but the enhancement at the emission maximum (598 nm) was only about 2.5 times. It is not clear why the enhancement is so much less than the Rh6G, but may be related to the overlap of the excitation wavelength (495 nm) and the resonance observed in the p-Si. Some of the excitation light is undoubtedly lost into the tail of the p-Si absorption.

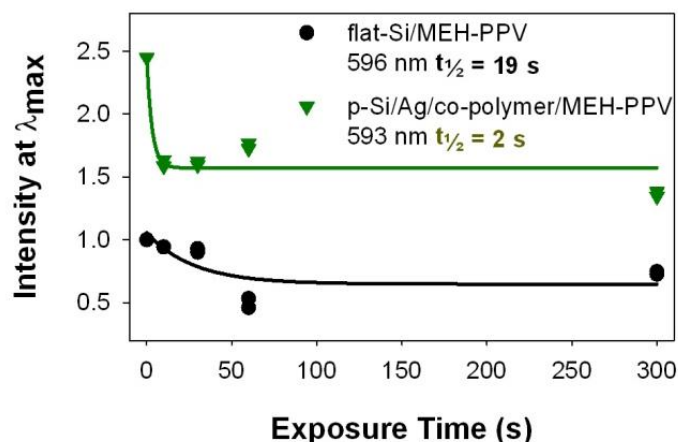


Figure 5. Quenching of MEH-PPV at λ_{\max} (598 nm) upon exposure to TNT, Black circles – flat Si/MEH-PPV; black line – exponential fit with half-life = 19 s; green triangle – p-Si/Ag/co-polymer/MEH-PPV; green line – exponential fit with half-life 2 s. Intensities are normalized to the flat-Si/MEH-PPV value at $t = 0$ s.

Figure 5 shows the effect of exposing flat-Si/MEH-PPV and p-Si/Ag/co-polymer/MEH-PPV samples to TNT. The decay of the emission maximum is plotted as a function of exposure time to vapors of TNT (formed from the natural vapor pressure of TNT at room temperature, which is in the ppb range). Both samples exhibit a quenching of about 60 % of the initial signal. Notably, the p-Si/Ag/co-polymer/MEH-PPV sample achieves this quenching significantly faster: the half-life for the flat-Si/MEH-PPV sample is 19 s while the half-life for the p-Si/Ag/co-polymer/MEH-PPV sample is only 2 s, nearly an order of magnitude improvement.

Conclusions

In conclusion, we have shown that by adding a light trapping layer to a MEF structure can increase the fluorescence signal intensity by a factor of several hundred

to over 1000. Further, when the light trapping layer is used in a TNT sensor, the signal intensity increases and the exposure time to reach maximum quenching is reduced, both qualities that are required for improved sensors. Work to better understand the influence of all the parameters in the structures is underway.

Notes

The authors declare no competing financial interests.

Acknowledgement

We gratefully acknowledge the ALERT Center of Excellence sponsored by the Department of Homeland Security for funding this work.

References

1. Geddes, C. D. and Lakowicz, J. R.; *J. Fluoresc.*, **2002**, *12*, 121 – 129.
2. Geddes, C. D.; Cao, H.; Gryczynski, I.; Gryczynski, Z.; Fang, J.; and Lakowicz, J. R.; *J. Phys. Chem. A*, **2003**, *107*, 3443 – 3449.
3. Parfenov, A.; Gryczynski, I.; Malicka, J.; Geddes, C. D.; and Lakowicz, J. R.; *J. Phys. Chem. B*, **2003**, *107*, 8829 – 8833.
4. Lakowicz, J. R.; *Anal. Biochem.*, **2005**, *337*, 171 – 194.
5. Aslan, K.; Leonenko, Z.; Lakowicz, J. R.; and Geddes, C. D.; *J. Phys. Chem. B*, **2005**, *109*, 3157 – 3162.
6. Deng, W. and Goldys, E. M.; *Langmuir*, **2012**, *28*, 10152 – 10163.
7. Gill, R.; Tian, L.; Somerville, W. R. C.; Le Ru, E. C.; van Amerongen, H.; and Subramanian, V.; *J. Phys. Chem. C*, **2012**, *116*, 16687 – 16693.
8. Guzatov, D. V.; Vaschenko, S. V.; Stankevich, V. V.; Lunevich, A. Y.; Glukhov, Y. F.; and Gaponenko, S. V.; *J. Phys. Chem. C*, **2012**, *116*, 10723 – 1073.
9. Levitsky, I. A.; Euler, W. B.; Tokranova, N.; and Rose, A.; *Appl. Phys. Lett.*, **2007**, *90*, 041904/1 – 041904/3.
10. Zeiri, L.; Rechav, K.; Porat, Z.; Zeiri, Y.; *Appl. Spec.*, **2012**, *66*, 294 – 299.
11. Saison-Francioso, O.; Lévêque, G.; Akjouj, A.; Pennec, Y.; Djafari-Rouhani, B.; Szunerits, S.; and Boukherroub, R.; *J. Phys. Chem. C*, **2012**, *116*, 17819 – 17827.